

# Magnetic structure of the southern Boso Peninsula, Honshu, Japan, and its implications for the formation of the Mineoka Ophiolite Belt

Toshiya Fujiwara<sup>1</sup>, Hajimu Kinoshita<sup>1</sup>, and Rie Morijiri<sup>2</sup>

<sup>1</sup>Deep-Sea Research Department, Japan Marine Science and Technology Center, 2-15, Natsushima-cho, Yokosuka 237-0061, Japan

<sup>2</sup>Geophysics Department, Geological Survey of Japan, 1-1-3, Higashi, Tsukuba 305-8567, Japan

(Received February 13, 1998; Revised June 4, 1999; Accepted June 17, 1999)

We conducted onshore and offshore magnetic surveys on and around the southern Boso Peninsula, Honshu, Japan, and observed prominent large amplitude anomalies along the Mineoka Ophiolite Belt, and long wavelength low anomalies to the south of the belt containing short wavelength isolated anomalies. The magnetic structure was modeled by using three-dimensional magnetic prisms and basement with about 1 A/m of magnetization. At the Mineoka Belt, the top of the magnetic prisms is located at the ground surface, and these bodies are elongate in the vertical direction, with high angle magnetic inclinations. Magnetic basement exists at shallow depth beneath the belt. The magnetic basement traces the bottom surfaces of the magnetic prisms and forms a graben structure. In the south of the Mineoka Belt, thin sheet-like magnetic prisms with low magnetic inclinations are assumed at 1–3 km depth. The magnetic structure implies the tectonic process of the formation of the Mineoka Ophiolite Belt. The belt could be fragmented pieces of an oceanic plate emplaced at a paleo-plate boundary, which originated in low latitude and was transported by obduction to the present place via northward drift.

## 1. Introduction

A characteristic feature of the surface geology in the southern Boso Peninsula, Honshu, Japan, is the existence of outcrops of ophiolitic rocks in the Mineoka Belt (Fig. 1). The Mineoka Ophiolite Belt consists mainly of pillow lavas, serpentized ultramafic and mafic rocks and their brecciated cumulates. The main body of outcrops is restricted to a narrow band with a length of about 10 km in east-west extent, starting at the east coast of the peninsula, and with a north-south width of less than 1 km (e.g. Kanehira *et al.*, 1968; Kanehira, 1976). Ophiolitic rocks crop out intermittently in the Hota or Hayama Belt from the Boso Peninsula to the Miura Peninsula (e.g. Uchida and Arai, 1978; Arai *et al.*, 1990). The ages of the Mineoka, Hota, and Hayama belts range from Paleogene to early Miocene and are older than the surrounding Miocene to Pliocene geological belts (GSJ, 1982). The age of basaltic rocks sampled at the Mineoka Ophiolite is estimated to be 30–50 Ma from K-Ar and Ar-Ar dating (Takigami *et al.*, 1980; Kaneoka *et al.*, 1981).

The line connecting the ophiolite outcrops is assumed to be a paleo plate boundary. The mechanism of emplacement of the ophiolitic rocks in the present location, between the northern tip of the Philippine Sea Plate and the Honshu landmass, must relate to the evolution of the trench-trench-trench type triple junction, located southeast of the Boso Peninsula (Fig. 1), and thus are important for understanding the paleo plate tectonics around the Japanese islands. Many arguments have been made about the origin and emplacement of the ophiolitic rocks and the related paleo plate tectonics (e.g.

Tonouchi and Kobayashi, 1983; Ogawa and Fujioka, 1985; Ogawa and Taniguchi, 1987; Arai, 1991; Arai and Okada, 1991; Soh *et al.*, 1991). Ogawa and Taniguchi (1987) proposed the existence of a Mineoka Microplate which developed through collision of the Izu island-arc with the Honshu landmass. Taira *et al.* (1989), and Arai and Okada (1991) suggested that the Mineoka Belt was formed by accretion of serpentine diapirs in the forearc region of the Izu-Bonin Ridge. Soh *et al.* (1991) proposed that the Mineoka Belt was produced by tectonic fragmentation of the crust of the Izu-Bonin Arc during arc-arc collision. Tectonic and petrographical studies of the Mineoka Ophiolite Belt and its surrounding area indicate that the Mineoka ultramafic body is a group of isolated and fragmented small bodies resulting from intrusion of serpentized gabbroic sheets in the Cenozoic era (Arai, 1991; Arai and Okada, 1991).

In spite of this accumulation of information, however, stratigraphic correlation between individual outcrops is poorly known because their outcrops are limited in size. Detailed subsurface structure of the southern Boso Peninsula can give an insight into the tectonics. Magnetic anomaly analysis is an effective tool for investigating the subsurface structure of this ophiolite belt because ophiolitic rocks carry strong magnetization in contrast to sedimentary layers. Aeromagnetic surveys have been carried out by a number of institutions and organizations (GSJ, 1980; JICA, 1983; NEDO, 1983; for compiled maps, Nakai *et al.*, 1987; GSJ and CCOP, 1996). A remarkable feature on the aeromagnetic anomaly maps is a magnetic low anomaly of –300 nT in amplitude extending in the SE-NW direction from off the Boso Peninsula to the Miura Peninsula (Fig. 2). This low anomaly belt traces the south edge of the ophiolitic rock outcrops,

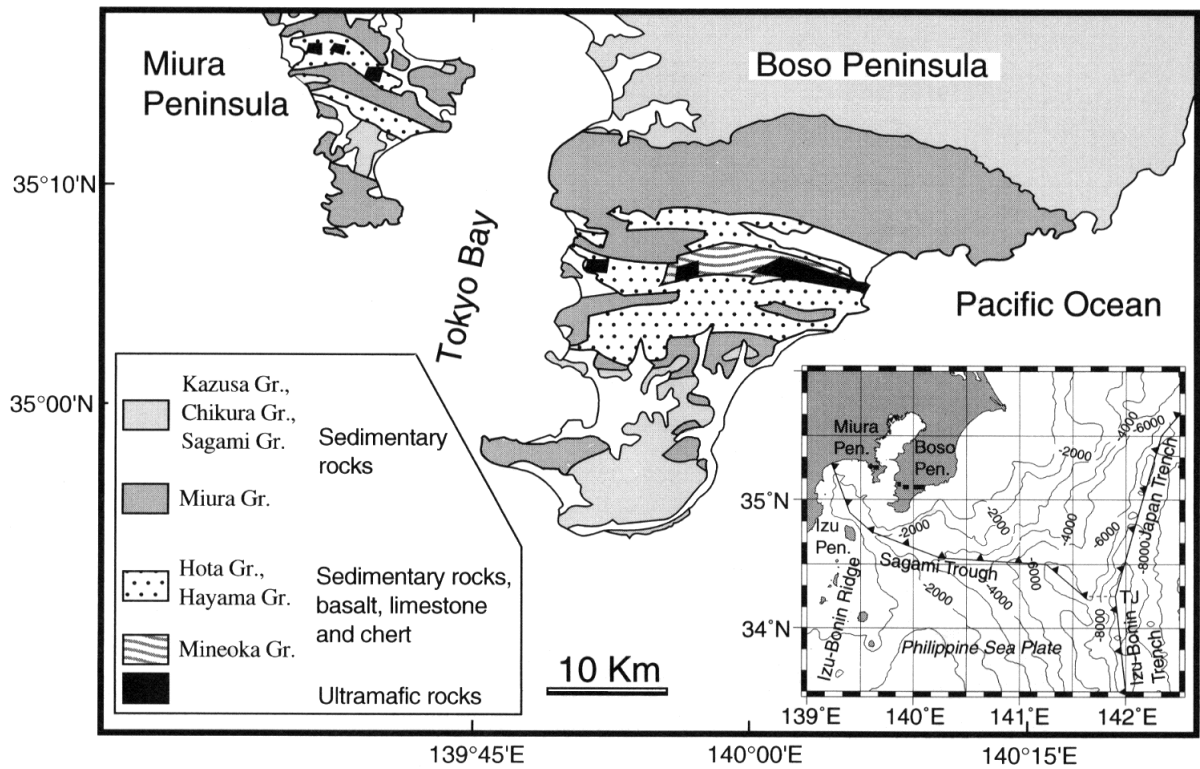


Fig. 1. Schematic geological map of the study area reproduced from Saito (1992). Areas filled black show outcrops of ophiolitic rocks. The inset shows a regional tectonic map of the study area. Bathymetric data are from Komazawa and Kishimoto (1995). Solid lines with triangles show plate subduction zones. Thick solid lines on the Boso and Miura peninsulas show approximate location of outcrops of ophiolitic rocks; TJ = Trench triple junction.

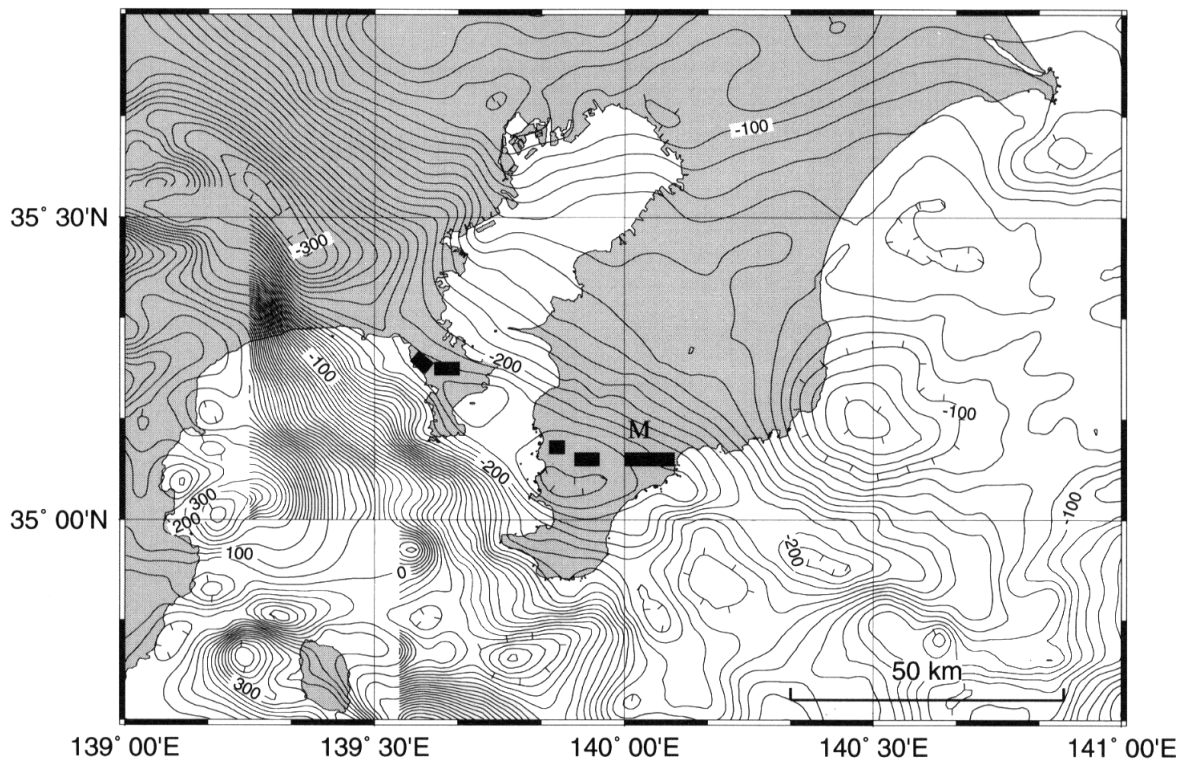


Fig. 2. Regional magnetic anomaly map from GSJ and CCOP (1996). Contour interval is 10 nT; M = Mineoka Belt.

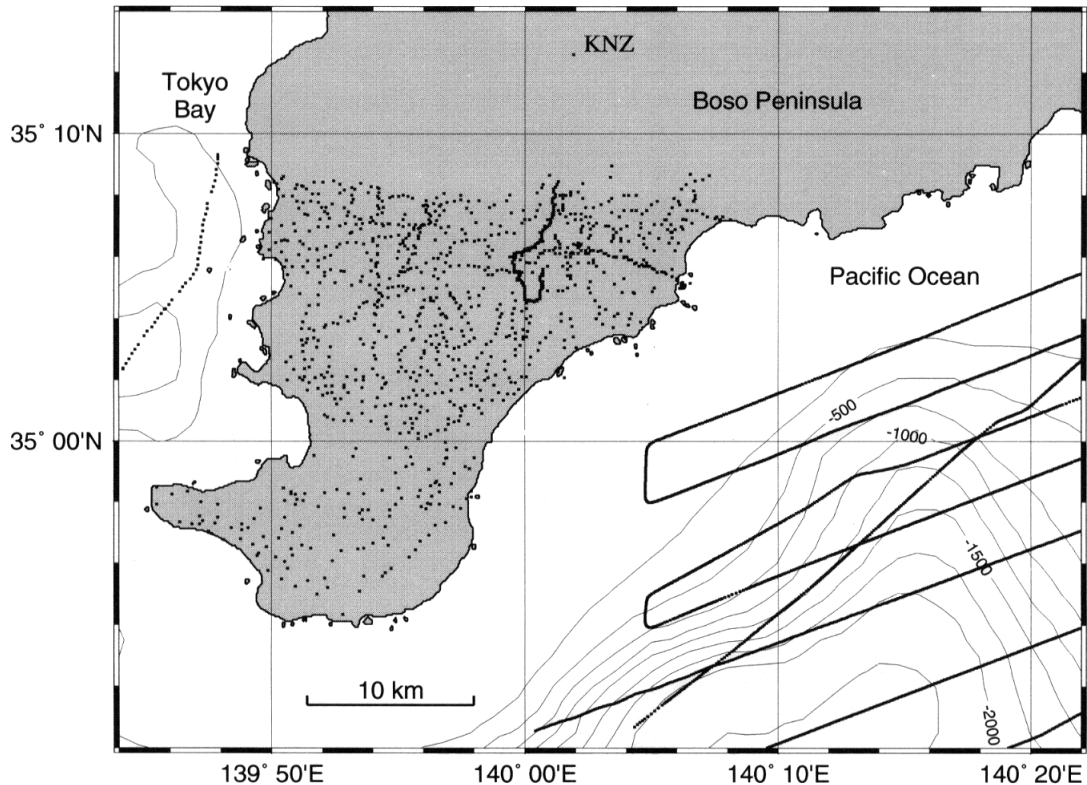


Fig. 3. Distribution of the magnetic observation points. Dot marks indicate the observation points. KNZ = Kano-zan Geodetic Observatory.

suggesting a relation between the magnetic anomaly and the structure of the ophiolitic belts. Tonouchi and Kobayashi (1983) discussed the Mineoka Ophiolite as the source of this low magnetic anomaly belt and proposed the subsurface structure. However, aeromagnetic anomalies are not of sufficient resolution for discussion of the magnetic structure of the Mineoka Ophiolite Belt. These aeromagnetic surveys, flown at 10,500 ft (3,200 m) above sea level, are made at a great distance from the magnetic source, and are not able to detect the magnetic anomalies due to the ophiolitic belt. The structure may be as small as the size of outcrops of the Mineoka Ophiolite; limited to a few kilometers. Because high resolution magnetic anomaly data were required to resolve this structure, we carried out ground magnetic surveys onshore and offshore of the southern Boso Peninsula to clarify the magnetic crustal structure.

## 2. Magnetic Data Collection

### 2.1 Magnetic surveys

The magnetic surveys on ground were carried out from 1985 through 1989. The measurements were made with a portable proton precession magnetometer Geometrics G-816 with a sensor height of 1.6 meters from the ground. Observation points were distributed from the southern end of the Boso Peninsula to 35°09'N (Fig. 3). We placed the observation points at intervals of 500 m. In some places where we found bare rock outcrops of the ophiolite, the points were picked up at 100 m interval. Of 1,212 observations made, 403 were run between midnight and dawn to avoid field dis-

turbances from electric railway activities near the survey area (Morijiri, 1988; Fujiwara, 1990). Magnetic data along a ship track in Tokyo Bay were obtained during the DELP 1987 Ogasawara cruise in November 1987 (Isezaki *et al.*, 1989). The magnetic total intensity anomaly was calculated by subtracting International Geomagnetic Reference Field (IGRF) 1985 model (IAGA, 1985) from the observed data. Diurnal variation of the geomagnetic field was corrected by using total geomagnetic intensity data measured every minute at the Kano-zan Geodetic Observatory, Geographical Survey Institute of Japan (139°57.5'E, 35°15.7'N) which was the nearest geomagnetic station and was located 7–34 km from the survey area. An upward continuation filter (Kato, 1987) was applied to eliminate anomalies due to artificial materials and to reduce topographic effects on the magnetic anomaly.

Sea-surface surveys of magnetics as well as swath bathymetry and gravity to the southeast of the Boso Peninsula were conducted aboard the R/V Yokosuka during the cruise YK98-02 Leg 1 in 1998. Total intensity and three-component geomagnetic field data were collected in this survey. The survey ship tracks trend in an ENE-WSW direction (Fig. 3). The interval of the northern tracks is about 4 km, and that of the southern tracks is about 6 km (Fujiwara *et al.*, 1998). Magnetic total intensity and vector anomalies were calculated by subtracting the IGRF 1995 (IAGA, 1995) from the data. The processing of the magnetic three-component data was accomplished using the method of Isezaki (1986). Correction of diurnal variation and upward continuation were not applied for this sea-surface magnetic data.

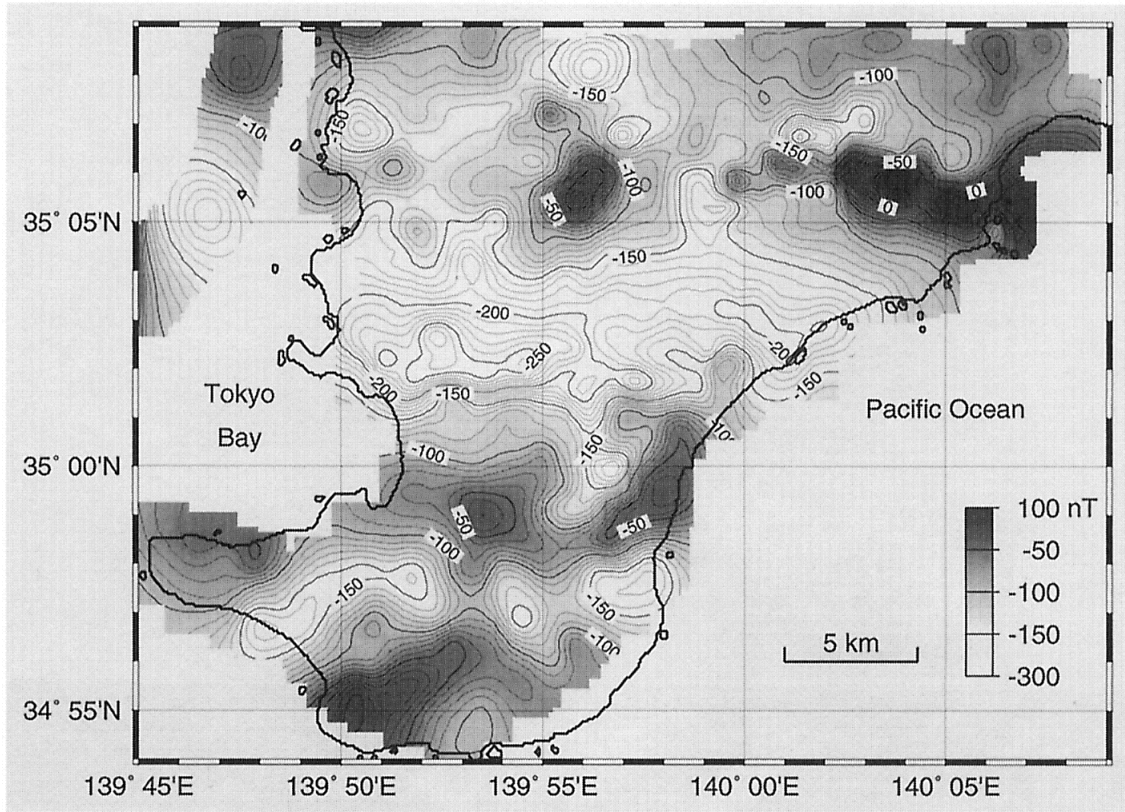


Fig. 4. Magnetic anomaly map continued to a height of 460 m (1,500 ft). Contour interval is 10 nT. High anomaly is shaded.

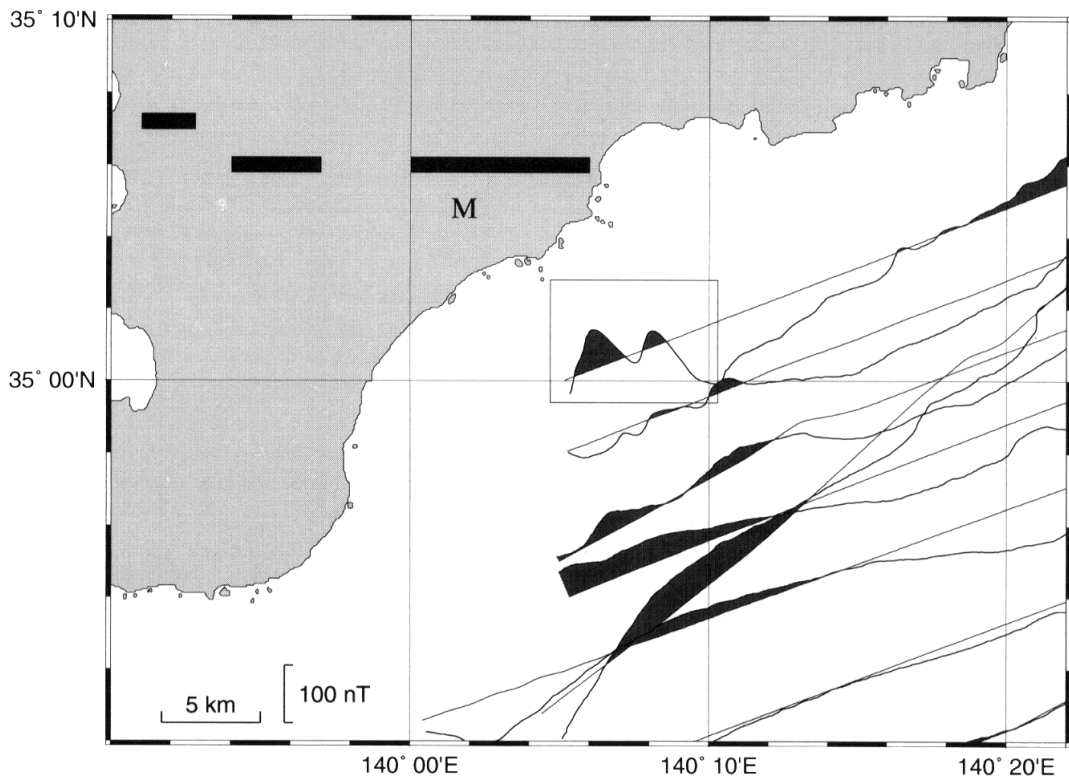


Fig. 5. Magnetic total field anomaly profiles along ship tracks. Anomalies, higher than the average value of  $-107$  nT in this area, are shaded. The box indicates the magnetic anomaly which is the subject of analysis in this study shown in Fig. 9.

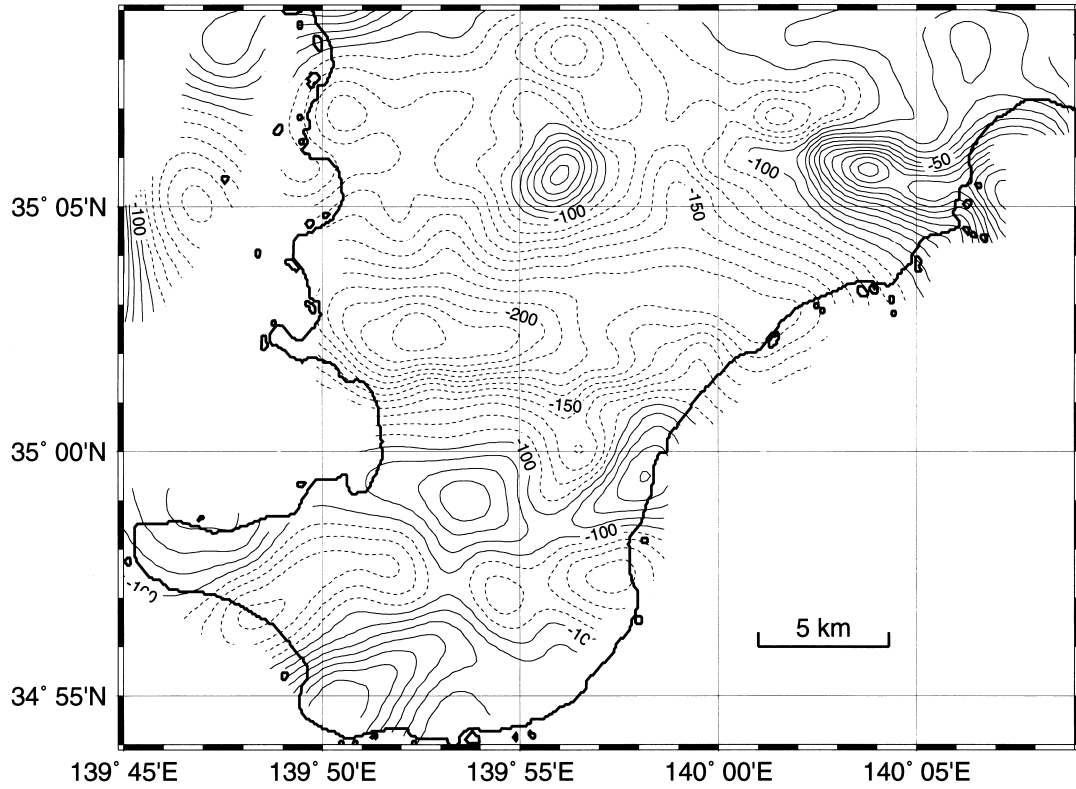


Fig. 6. Magnetic anomaly map continued to a height of 1,000 m. Contours of solid lines show values of higher than  $-100$  nT, and contours of dashed lines show values of lower than  $-100$  nT. Contour interval is 10 nT.

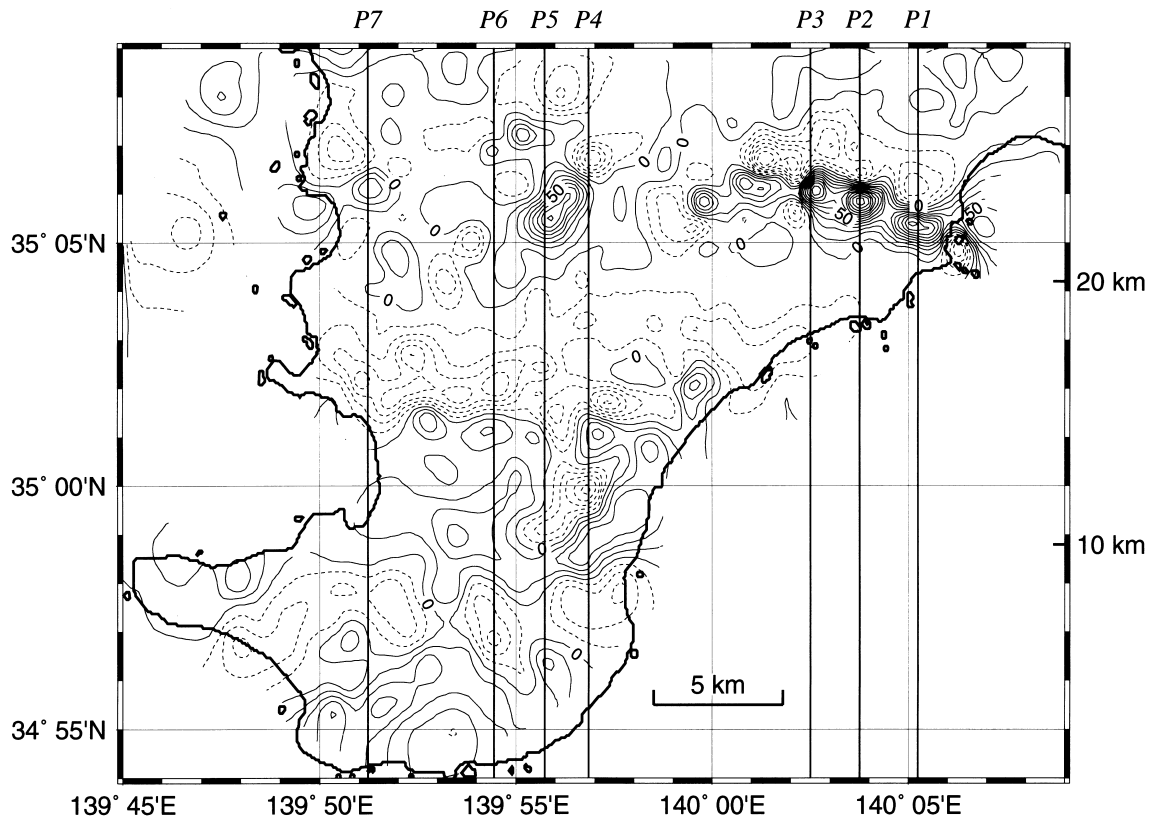


Fig. 7. Residual magnetic anomaly map obtained by subtracting the anomaly at the height of 1,000 m from the anomaly on the height of 460 m. Contours of solid lines show positive values (high anomaly), and contours of dashed lines show negative values (low anomaly). Contour interval is 10 nT. Solid lines show the profiles for forward modeling.

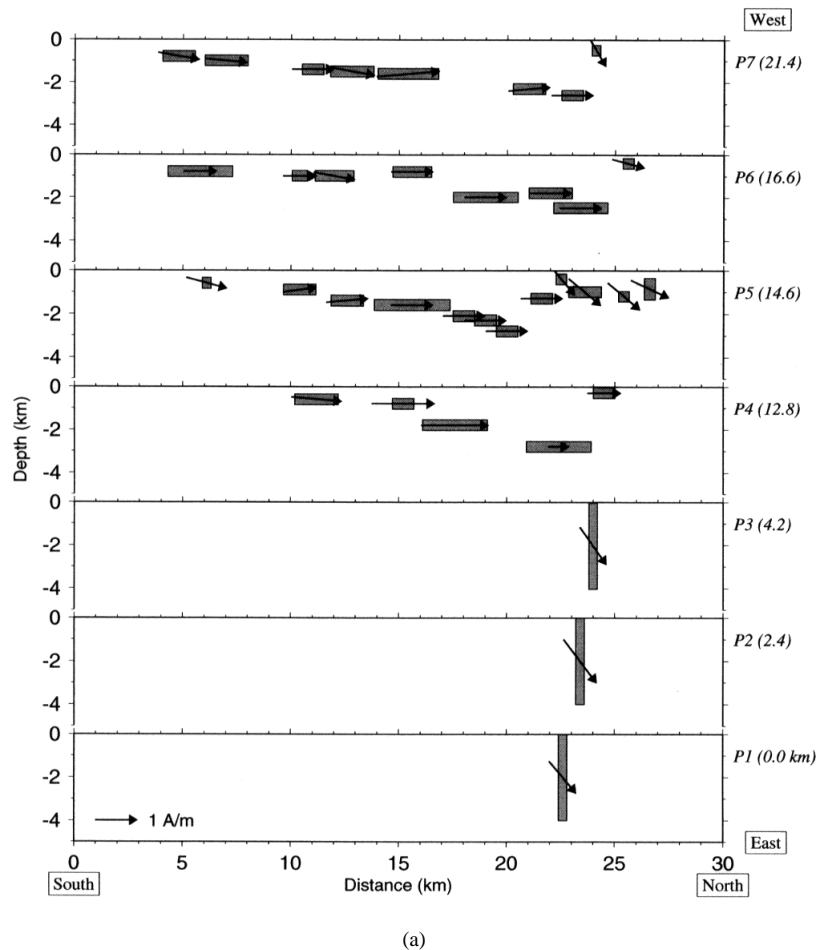


Fig. 8. (a) north-south cross sections of the prism-shaped models which satisfy the short wavelength magnetic anomalies. Vertical axes indicate depth below the ground surface. Rectangles indicate the location and size of the magnetic prisms. The arrow length shows the relative magnetization intensity and the arrow direction indicates the inclination. Values in parentheses shows distances in km from P1. (b) comparison between the observed (plain) and the calculated anomaly profiles (bold).

## 2.2 Magnetic anomaly

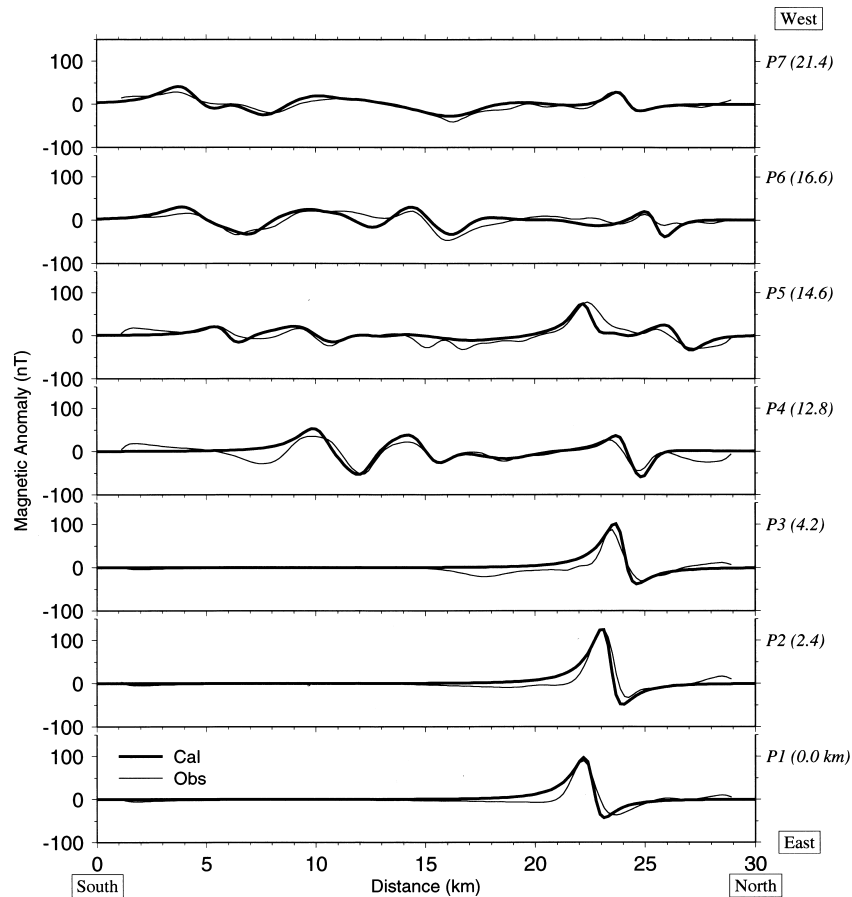
The magnetic anomalies as measured on the ground and continued upward 460 m (1,500 ft) are shown in Fig. 4. The height of 460 m is chosen in order to even out the data density while preserving the characteristic high resolution. This height is also convenient for comparing with aeromagnetic maps measured over the offshore areas (GSJ, 1980; JICA, 1983). The magnetic anomalies on the peninsula reveal that a number of conspicuous isolated highs and lows are superimposed on a long wavelength anomaly pattern which has an east-west strike direction; the highest anomaly group is aligned along the ophiolitic rock outcrops, high anomalies are dominant to the south of  $35^{\circ}00'N$ , and low magnetic anomalies are distributed between these high anomalies.

The sea-borne magnetic anomalies feature a low anomaly belt extending in the ESE-WNW direction with high anomalies surrounding it (Fig. 5). The general trend is correlated well with the published magnetic anomaly map (GSJ and CCOP, 1996). High anomalies with short wavelength and large amplitude, which do not appear on the published map, were observed at  $140^{\circ}07'E$ ,  $35^{\circ}01'N$  in the south of the Mineoka Belt.

## 3. Data Analysis

### 3.1 Analysis of the on-land magnetic anomaly

The power spectrum of the observed magnetic anomalies took the form of two straight-line segments with a change in slope at a wavelength of about 4 km, and thus the magnetic data were divided into shorter and longer wavelength anomalies for analysis of the magnetic anomaly on land. The short and long wavelength anomalies were considered to be attributable to local and regional structure, respectively. The upward continuation technique was used to divide wavelength elements in this study. Low-pass magnetic anomalies were obtained by upward continuation to a height of 1,000 m (Fig. 6). High-pass magnetic anomalies were obtained by subtracting magnetic anomalies at a height of 1,000 m from magnetic anomalies at a height of 460 m (Fig. 7). The two wavelength anomaly components were analyzed by different techniques. The residual short wavelength anomalies are supposed to be due to isolated three-dimensional bodies of magnetic rock in relatively non-magnetic sedimentary layers in shallow depths. Natural remanent magnetization with arbitrary polarization may be strong. Induced magnetization as well as remanent magnetization is of importance for the regional structure. The magnetic induction vector varies lit-



(b)

Fig. 8. (continued).

tle in this region, so it is a large contribution to the sum total of magnetization of the regional structure. Vectors of natural remanent magnetization of small crustal blocks often have random orientation because of migration or rotation caused by crustal movement.

### 3.2 Modeling for short-wavelength magnetic anomaly

The residual short-wavelength anomalies are modeled by forward calculation using magnetized rectangular prisms; this allows arbitrary polarization of magnetization to be taken into account (Fujiwara, 1990; Fujiwara *et al.*, 1990; Ogura, 1990). The simplest model among three-dimensional models is chosen because we have no constraint on the detailed crustal structure. The magnetic anomaly due to rectangular prisms was calculated by using the method of Bhattacharyya (1964). The ambient geomagnetic field was assumed to be parallel to the IGRF 1985 field which had a declination of  $-6^\circ$  and inclination of  $48^\circ$  in the study area. Parameters in the forward modeling include length along the profile, width across the profile, thickness, depth, magnetization (declination, inclination, and intensity), and position of a prism. Observed magnetic anomaly wavelengths in the east-west direction are relatively constant compared to that in the north-south direction (Fig. 7). The width of all prisms was set to 2 km. The declination of each prism was determined by inferring the direction from peak to bottom positions of isolated anomalies. The other parameters for each prism were

estimated from the isolated magnetic anomaly patterns by trial and error. The information sought was derived via the following procedure. The position of the magnetic prism was inferred from the distribution of the magnetic anomaly. The length in the north-south direction was estimated from the wavelength of the anomaly. The top depth to the magnetic prism was estimated from the waveform of the anomaly. The magnetization intensity was deduced from the amplitude of the anomaly. The ratio of high to low anomalies gave information on magnetic inclination. Finally, the thickness of the magnetic prism was controlled to find the best match to the waveform of the observed magnetic anomaly. No topographic correction was applied because most of the surface geology consisted of sediment layers with weak magnetization.

Seven profiles were selected as shown in Fig. 7. Profiles 1 to 3 cross over the Mineoka Ophiolite Belt. Because the magnetic anomalies are considered to be produced by the ophiolitic rocks, magnetic prisms are placed beneath the Mineoka Ophiolite Belt with upper surfaces that are constrained to be at the ground surface (Fig. 8(a)). The length in the north-south direction is estimated to be 500 m from the wavelength of the anomalies, which is almost the same size as the outcrops of ophiolitic rocks. Magnetization intensities were adjusted from 1 to 1.5 A/m to match anomaly amplitudes (Fig. 8(a)). The shape of isolated magnetic anomalies

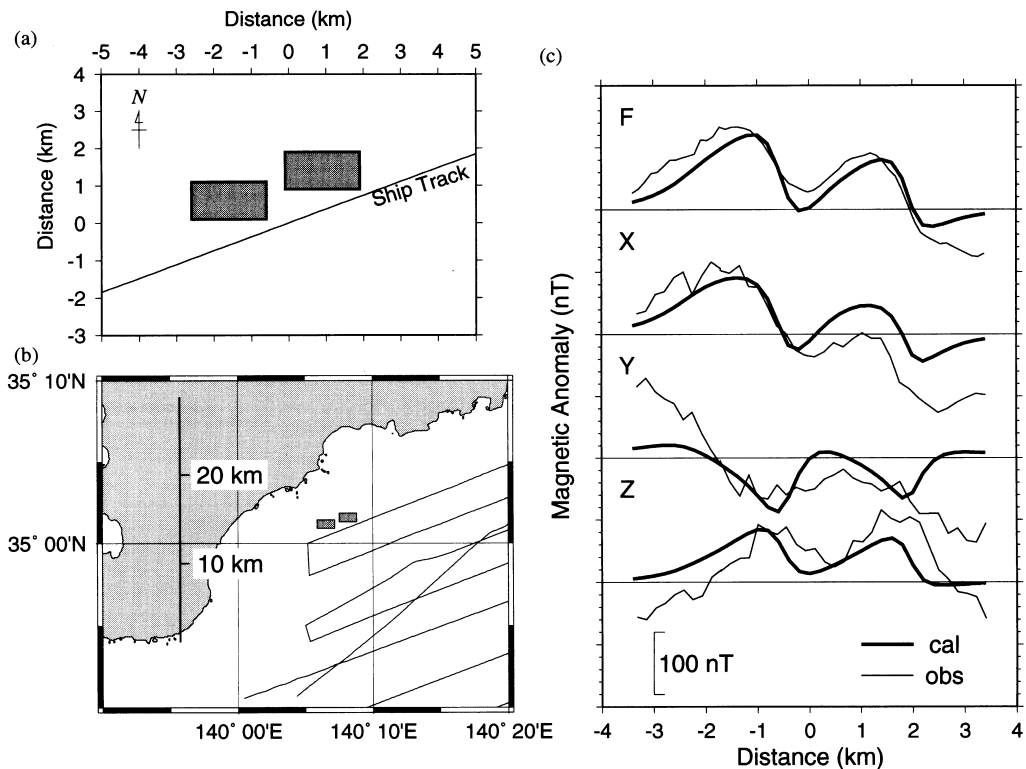


Fig. 9. (a) overview of prism-shaped models which satisfy the sea-surface magnetic anomalies. Magnetized prisms extend 1 km in the north-south direction, 2 km in the east-west direction, and have thickness of 0.5 km. (b) magnetized prisms are located to the north of the ship track, at around 15 km in distance in reference to the profiles of Fig. 8. (c) comparison between the observed (plain) and calculated anomaly profiles (bold); F = total force, X = northward component, Y = eastward component, Z = downward component.

shows prominent high and small low anomaly amplitudes (Fig. 8(b)), so we set magnetized inclinations to high angles, ranging from  $50$  to  $60^\circ$ , and set bottom surfaces of the prisms to depths of 4,000 m.

For the analysis of Profiles 4 to 7, the length in the north-south extent and the depth to the top of prisms are varied to adjust the wavelengths and the waveforms. The shape of isolated magnetic anomalies shows that amplitudes of low anomaly are larger than that of high anomaly of this pair, thus the magnetic inclinations seem to be low (Fig. 8(a)). The initial magnetization intensity was assumed to be 1 A/m, the same as the value used for Profiles 1 to 3. Resultant magnetization intensities range from 0.5 to 1.5 A/m. The observed magnetic anomalies are fit well by assuming magnetized prisms with 500 m thickness (Fig. 8(b)). The solutions reveal that arrays of sheet-like magnetic prisms are extending horizontally. The depth of these magnetic prisms increases by about 3,000 m from south to north, while the magnetic prisms are at shallow depth beneath the Mineoka, Hota, and Hayama belts.

### 3.3 Modeling for sea-borne magnetic anomaly

The vector magnetic anomalies, located at  $140^\circ 07'E$ ,  $35^\circ 01'N$ , were analyzed using magnetic prism models (Fig. 9). The ambient geomagnetic field was set to declination of  $-7^\circ$  and inclination of  $48^\circ$  based on IGRF 1995. Two prisms were assumed because two peaks were observed. An east-west extent of 2 km for the magnetic prisms is constrained by the wavelength of the anomalies. The relatively

small amplitude eastward component (Y) of the anomaly indicates that magnetized inclinations are low angle. A westward shift of declination is necessary to adjust the positions of peaks of each component of the anomalies. Therefore magnetization directions of  $-30^\circ$  in declination and  $0^\circ$  in inclination are assumed. The location and dimension of the magnetic prisms are poorly constrained because we have data along only one track. The probable resultant magnetic structure is two prisms located to the north of the ship track. Provided that the upper surface of the prisms is the seafloor, their thickness would be 500 m, the length in north-south extent would be 1 km, and the magnetization intensities would be 1.0 and 1.7 A/m.

### 3.4 Modeling for long-wavelength magnetic anomaly

Magnetic basement undulation for the regional structure was inferred from magnetic anomalies continued to a height of 1,000 m by using two-layer model inversion. The method is carried out using pseudogravity and reduction to the pole anomalies derived from observed total intensity anomalies. Magnetic anomalies are inverted assuming that anomalies are caused by undulations of the interface between the two layers in a model consisting of a surface layer and an underlying magnetized layer (Okuma *et al.*, 1989). As for parameters of the analysis, mean depth of the magnetic basement is derived from least square fitting of the slope of the power spectrum of the reduction to the pole anomaly (Chenot and Debeglia, 1986). The mean depth was assumed to be 2,000 m below the ground surface in this study. The direction of ambient



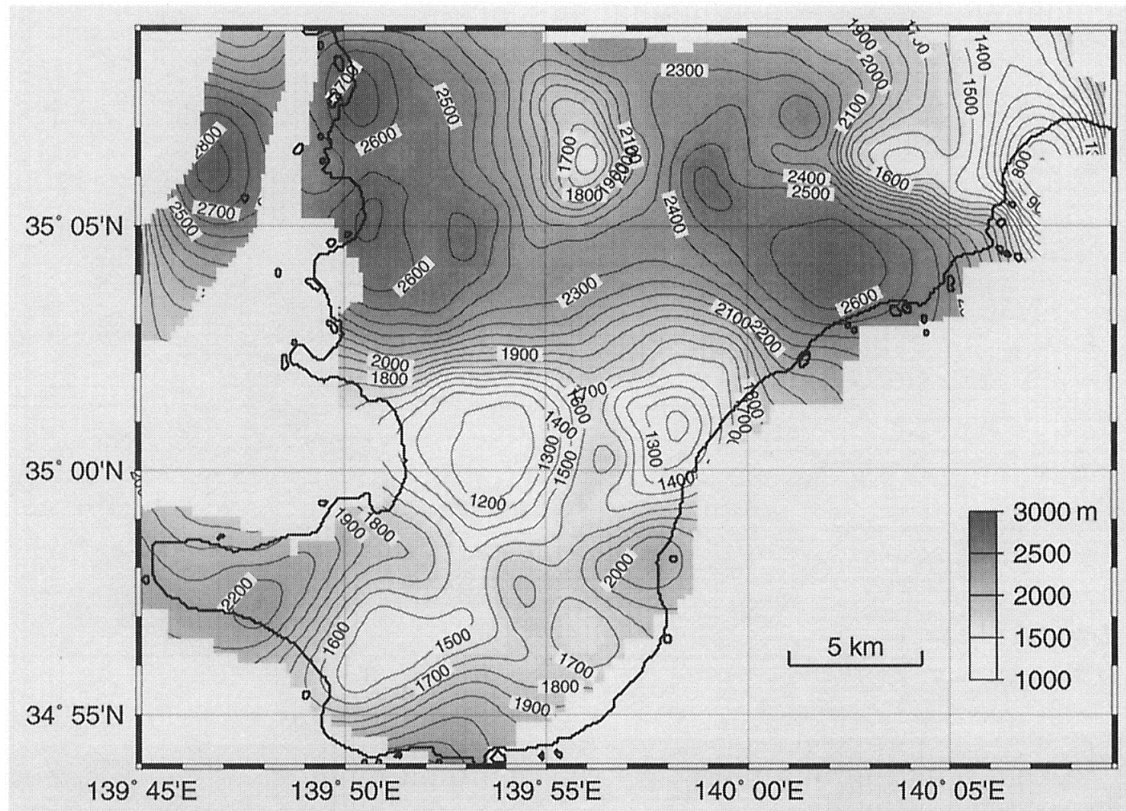


Fig. 10. Magnetic basement depth map. Contour interval is 100 m. The area of relatively deep basement is shaded.

geomagnetic field was fixed to a declination of  $-6^\circ$  and an inclination of  $48^\circ$  based on IGRF 1985. Direction of magnetization is assumed to be parallel to the ambient geomagnetic field. The magnetization intensity contrast was set to 1 A/m based on the results of forward modeling.

Figure 10 is a map of the magnetic basement undulation derived from the two-layer inversion. Depth of magnetic basement ranges from 1 to 3 km below the ground surface. The magnetic basement is shallow beneath the southern study area. The basement is also shallow beneath the Mineoka Ophiolite Belt. This shallow basement is considered to be the source of high magnetic anomalies. The magnetic basement is deep and shows graben structure in the northern study area. There is a step-like increase in depth from south to north across  $35^\circ 02' N$ . The abrupt depression of the basement causes the low magnetic anomaly extending in an east-west direction (Fig. 6).

#### 4. Discussion

##### 4.1 Comparison between the resultant magnetic structure and previous geophysical studies

Our magnetic modeling shows that appropriate mean magnetization of the magnetic source rocks in this region is 1 A/m. The mean magnetized intensity is consistent with the following paleomagnetic results from the Mineoka Ophiolite Belt (Tonouchi and Kobayashi, 1983): the natural remanent magnetization of pillow basalts of 0.3–8.8 A/m, dyke basalts of 0.2–4.1 A/m, and serpentinized rocks of 0.8–1.4 A/m. The arithmetic mean of magnetization intensity of all samples of 1.7 A/m is roughly comparable to our estimate of in situ

magnetization of the ophiolitic bodies. The Königsberger ratio averages 3.2 for pillow basalts, indicating that natural remanent magnetization dominates induced magnetization in magnetic anomalies locally. The Königsberger ratios are 0.8 for dolerite, 1.1 for gabbro, and 0.5–6.1 for ultramafic rocks, thus induced magnetization is considered to be a significant component for the bulk of the ophiolitic rocks. If a weak magnetization contrast is assumed, it makes a large amplitude undulation of the magnetic basement. For the case of a magnetization contrast smaller than 0.5 A/m, the magnetic basement reaches the ground surface in the southern study area. Therefore the basement magnetization contrast must be larger than 0.5 A/m because there is no outcrop of ophiolitic rocks in the area.

Our results show that the Mineoka Ophiolite is elongate vertically from the ground surface, and can be modeled by vertical magnetic prisms and shallow magnetic basement. Therefore the structure is inhomogeneous horizontally beneath the Mineoka Belt (Fig. 11). In a previous study, Kinoshita *et al.* (1995) discussed the magnetic structure using a part of our geomagnetic data set, along a line of  $139^\circ 55' E$ . They modeled the Mineoka Ophiolite with a magnetic prism having a thickness of 500 m. However we argue that the ophiolite body has a much deeper root of about 4 km from the analysis shown in Profile 1 to 3 in Fig. 8. Aeromagnetic data suggest that the Mineoka Ophiolite magnetic body has a root not much deeper than several kilometers. The amplitude of the magnetic anomalies observed at ground level rapidly decrease at higher altitude, implying that the entire size of the ophiolite bodies is small and is confined in a narrow band.

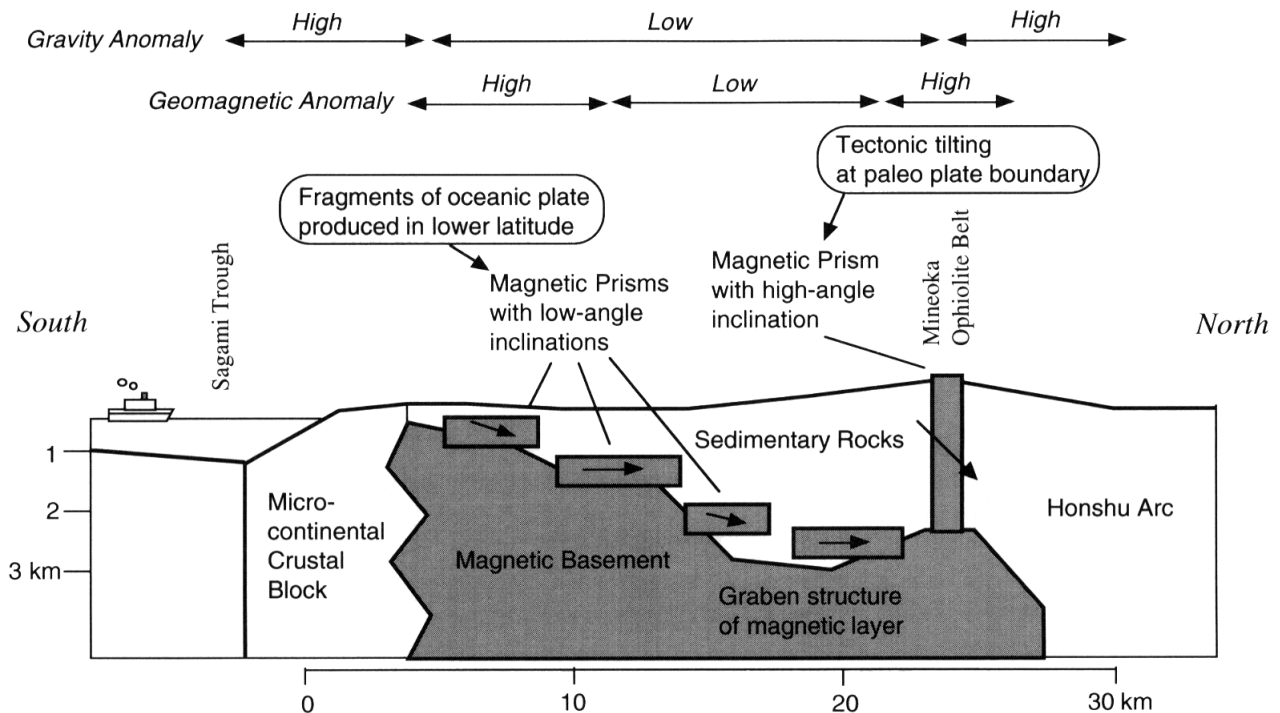


Fig. 11. Schematic north-south cross section of the magnetic structure and its tectonic interpretation for the formation of the Mineoka Ophiolite Belt and its adjacent area. Vertical exaggeration = 2.2.

We showed that it is possible to trace the continuation of the paleo plate boundary, which gives information regarding the evolution of the triple junction, by mapping magnetic anomalies with large amplitudes and short wavelengths. However, the eastern extension of the Mineoka Ophiolite Belt to the Pacific Ocean was not detected in spite of the sea-surface survey, probably because of the deep water depth or sparse interval of the ship tracks (Fig. 3).

Inhomogeneous horizontal structure beneath the Mineoka Belt is also suggested from seismic explosion experiments. There is an offset in the upper boundaries of seismic velocity layers beneath the Mineoka Belt (Asano *et al.*, 1979), and a seismic velocity discontinuity has an abruptly steep dip in the south of the Mineoka Belt (Hasegawa, 1988). These seismic velocity studies showed that there is a thick sedimentary layer to the south of the Mineoka Belt. This result is consistent with our magnetic structure having graben structure. Morijiri *et al.* (1990) and Kinoshita *et al.* (1995) argued that there was a gap in the magnetic basement, and inferred a non-magnetic layer there to explain the low magnetic anomaly. These seismic studies, however, show no evidence of structural discontinuity.

There is the possibility of a lateral change in structure beneath Sagami Bay to the southwest off the Boso Peninsula (Asano *et al.*, 1979). This velocity discontinuity is also inferred from the observation of earthquake swarms (Mizoue *et al.*, 1981). These results may show that the presumable basement of the southern tip of the Boso Peninsula is isolated from the surrounding basement. The Bouguer gravity anomaly shows a local peak of high anomaly, which shows a circular shape with a radius of about 30 km centered to the south off the Boso Peninsula (Ueda *et al.*, 1987; Kono

and Furuse, 1989). The gravity anomaly high extends in an east-west direction to the north of the Mineoka Belt. A low gravity anomaly is located in the study area between the high anomalies. The gravity anomaly structure supports the existence of a sedimentary layer, lying between relatively high density crustal blocks.

#### 4.2 Implications for the formation of the Mineoka Ophiolite Belt

The magnetized vectors of the modeled magnetic prisms deviate from the ambient geomagnetic vector, suggesting that these magnetic prisms have strong natural remanent magnetization. The less than 1 km thickness and length scale of the magnetic prisms is consistent with a pillow basaltic layer of oceanic crust produced at an oceanic spreading center. In consideration of the geological setting of the study area, it is possible that the magnetic prisms represent fragments of a pillow basaltic layer. The magnetic basement is thus regarded as emplacement of an oceanic lower crust and a layer of serpentinized upper mantle rocks. The magnetic inclinations show low angles of 0–20° in the southern part of the study area. The paleomagnetic result from the southern part of Mineoka Hill also has systematically low inclinations from –20 to 20° (Tonouchi and Kobayashi, 1983). These inclinations are significantly low compared to 48° which is expected for the present position at 35°N, and suggest that the oceanic crust has been carried from a low latitudinal region. We cannot specify the precise paleo latitude because our result cannot constrain the original horizontal plane, but Tonouchi and Kobayashi (1983) discussed the paleo latitude from their paleomagnetic investigation. They concluded the inclination of 34° after bedding correction, thus the paleo latitude 23°N, which is about 1,000 km south of the present

location. The inclinations of the magnetic modeling show, in contrast, high angles of 50–60° beneath the Mineoka Belt consistent with the paleomagnetic measurements of 30–60° on the northside of Mineoka Hill (Tonouchi and Kobayashi, 1983). The high angle inclinations suggest that these fragments of oceanic crust are highly tilted and have been thrust to the ground surface by tectonic processes. This part of the crust seems to be undergoing active uplift that has formed a bulge of hills which are bounded on both sides by fault lines running almost east to west (Research Group for Active Faults of Japan, 1991).

The burial depth of the magnetic basement and prisms varies systematically (Figs. 8(a) and 11). The magnetic layers are buried shallow in depth in the southern part of the study area, and the burial depth increases by about 3,000 m from south to north in the middle of the study area. A possible interpretation of the origin of the northward dipping structure is that it is a relic of a slab slope of the paleo oceanic plate. The other possibility is that it is a product of successive uplifting of the southern part of the study area (Sugimura and Naruse, 1954, 1955).

A possible mechanism for emplacement of the oceanic crust is collision of a micro-continent and obduction of an oceanic plate. A micro-continental block may have collided with the Honshu Arc. The oceanic plate, existing between the two continental blocks, obducted on the landward slope along with accretionary sediments. Fragments of the oceanic plate are buried in accretionary sediments to the south of the Mineoka Belt. The Mineoka Ophiolite Belt was formed by fragments that were sandwiched and rotated to high angles in the compressive stress field at the paleo-plate boundary.

## 5. Conclusions

1. We conducted onshore and offshore magnetic surveys on and around the southern Boso Peninsula, Honshu, Japan, to investigate the magnetic crustal structure. The surveys revealed magnetic high anomalies, which have prominent large amplitudes and align along the Mineoka Ophiolite Belt, many isolated anomalies with short-wavelength were observed. The surveys also detected low anomalies extending in the WNW-ESE direction. This is a common feature in published aeromagnetic anomaly maps (e.g. Nakai *et al.*, 1987; GSJ and CCOP, 1996).

2. Magnetic structure along the Mineoka Belt is modeled by shallow magnetic basement and three-dimensional magnetic prisms with about 1 A/m of magnetization. The top of the magnetic prisms is located at ground level, and these bodies are elongate in the vertical dimension. The prisms have high angle magnetic inclinations.

3. Isolated anomalies distributed to the south of the Mineoka Belt are interpreted as thin sheet-like magnetic prisms with low magnetic inclinations and 1 A/m of magnetization. Their burial depth changes systematically; from shallow in the southern to deep in the northern area. The magnetic basement traces the bottom surfaces of the magnetic prisms and thus shows a graben structure running through the south of the Mineoka Belt and striking in an east-west direction.

4. We propose that the Mineoka Ophiolite Belt was formed from fragments of oceanic plate. The fragments of oceanic

plate originated at low latitude were emplaced at the paleo-plate boundary, and obducted on the landward slope along with accretionary sediments. These fragments of oceanic crust are highly tilted and have been thrust to the ground surface. Fragments of oceanic plate are buried in accretionary sediments in the south of the Mineoka Belt. The northward dipping structure reflects slab slope of the paleo oceanic plate or successive uplift of the southern part.

**Acknowledgments.** We would like to acknowledge T. Kanamatsu and T. Nagao who provided many stimulating scientific discussions. We are grateful to N. Isezaki, N. Seama, and M. Yamamoto, to the officers and the crew of the R/V Yokosuka for their assistance in collecting data during the YK98-02 Leg 1 cruise. We also acknowledge the Kano-zan Geodetic Observatory, Geographical Survey Institute which offered reference geomagnetic data. We thank R.W. Saltus and an anonymous referee, whose suggestions and comments were useful to improve the manuscript. Most of the figures have been generated using GMT (Generic Mapping Tool) (Smith and Wessel, 1990; Wessel and Smith, 1991).

## References

- Arai, S., M. Ito, N. Nakayama, and F. Masuda, A suspect serpentinite mass in the Tokyo Bay area: petrology and provenance of serpentinite pebbles in the upper Cenozoic system in the Boso Peninsula, central Japan, *J. Geol. Soc. Japan*, **96**, 171–179, 1990 (in Japanese with English abstract).
- Arai, S., *The Circum-Izu Massif Peridotite, Central Japan, as Back-Arc Mantle Fragments of the Izu-Bonin Arc System, Ophiolite Genesis and Evolution of the Oceanic Lithosphere, Proceedings of the Ophiolite Conference, Held in Muscat, Oman, 7–18 January 1990*, pp. 801–816, Kluwer Academic Publishers, Dordrecht, the Netherlands, 1991.
- Arai, S. and H. Okada, Petrology of serpentinite sandstone as a key to tectonic development of serpentinite belts, *Tectonophys.*, **195**, 65–81, 1991.
- Asano, S., Y. Ichinose, I. Hasegawa, S. Iizuka, and H. Suzuki, Crustal structure in the southern Kanto district derived from explosion seismic data, *J. Seismol. Soc. Japan*, **2**, **32**, 41–55, 1979 (in Japanese with English abstract).
- Bhattacharyya, B. K., Magnetic anomalies due to prism-shaped bodies with arbitrary polarization, *Geophys.*, **29**, 517–531, 1964.
- Chenot, D. and N. Debeglia, Gravity and magnetic 3-D interactive inversion with constraints, *56th Ann. Internat. SEG Mtg.*, Expanded abstracts with Biographics, 219–221, 1986.
- Fujiwara, T., Study of crustal structure in the southern part of Boso Peninsula inferred from magnetic anomalies and its tectonic implications, M.S. Thesis, Chiba Univ., 1990.
- Fujiwara, T., S. Ogura, R. Morijiri, and H. Kinoshita, The crustal structure of the southern part of Boso Peninsula based on magnetic anomaly study, *Rock Mag. Paleogeophys.*, **17**, 100–105, 1990.
- Fujiwara, T., N. Seama, M. Yamamoto, N. Isezaki, and H. Kinoshita, Geomagnetic survey of the off-Kamogawa, Boso Peninsula, Japan, *JAMSTEC J. Deep Sea Res.*, **14**, 467–476, 1998 (in Japanese with English abstract).
- Geological Survey of Japan (GSJ), *Off the Coast of Boso-Izu-Sagami Nada Area, Total Intensity Aeromagnetic Maps 1:200,000 Series No. 27*, 1980.
- Geological Survey of Japan (GSJ), *Geological Atlas of Japan*, 119 pp., 1982.
- Geological Survey of Japan (GSJ) and Coordinating Committee for Coastal and Offshore Geoscience Programs in East and Southeast Asia (CCOP), *Magnetic Anomaly Map of East Asia 1:4,000,000 CD-ROM Version*, 1996.
- Hasegawa, I., Structure of the pre-Tertiary basement beneath the Kanto Plain revealed by geophysical data, *Mem. Geol. Soc. Japan*, **31**, 41–56, 1988 (in Japanese with English abstract).
- IAGA Division I WG 1, International Geomagnetic Reference Field revision 1985, *J. Geomag. Geoelectr.*, **37**, 1157–1163, 1985.
- IAGA Division V WG 8, International Geomagnetic Reference Field, 1995 revision, *J. Geomag. Geoelectr.*, **47**, 1257–1261, 1995.
- Isezaki, N., A new shipboard three component magnetometer, *Geophys.*, **51**, 1992–1998, 1986.
- Isezaki, N., H. Inokuchi, H. Ishikawa, H. Ichikawa, K. Takahashi, Y. Inoue, and K. Sugimoto, Report on DELP 1987 cruises in the Ogasawara area Part V. Measurement of three components and total intensity of the geomagnetic field in the Ogasawara trough, *Bull. Earthq. Res. Inst., Univ. Tokyo*, **64**, 179–222, 1989.

- Japan International Cooperation Agency (JICA), *1:200,000 Total Intensity Aeromagnetic Map over the Uruga Strait*, 1983.
- Kanehira, K., Mode of occurrence of serpentinite and basalt in the Mineoka district, southern Boso Peninsula, *Mem. Geol. Soc. Japan*, **13**, 43–50, 1976 (in Japanese with English abstract).
- Kanehira, K., Y. Oki, S. Sanada, M. Yabe, and F. Ishikawa, Tectonic blocks of metamorphic rocks at Kamogawa, southern Boso Peninsula, *J. Geol. Soc. Japan*, **74**, 529–534, 1968.
- Kaneoka, I., Y. Takigami, S. Tonouchi, T. Furuta, Y. Nakamura, and M. Hirano, Pre-Neogene volcanism in the central Japan based on K-Ar and Ar-Ar analyses, in Abstracts 1981 IAVCEI Symposium—Arc Volcanism, Tokyo and Hakone, *Volcanol. Soc. Japan*, **166**, 1981.
- Kato, M., *Theory of Two-dimensional Filter and Analysis of Gravity and Magnetics, Lattice*, 262 pp., Lattice, Tokyo, 1987 (in Japanese).
- Kinoshita, H., Y. Nakasa, R. Morijiri, and T. Fujiwara, Formation of backarc basin and genesis of ophiolite, *J. Geography*, **104**, 392–407, 1995.
- Komazawa, M. and K. Kishimoto, Bathymetric data around Japan (1 km mesh), *News Lett. Seis. Soc. Japan*, **7**, 4, 3–4, 1995 (in Japanese).
- Kono, Y. and N. Furuse, *1:1 Million Scale Gravity Anomaly Map in and around the Japanese Islands*, Univ. Tokyo Press, Tokyo, 1989.
- Mizoue, M., I. Nakamura, H. Chiba, M. Yoshida, H. Hagiwara, and T. Yokota, The structure of the upper part of the crust in the regions of Sagami Bay, the Izu Peninsula and Suruga Bay as found by the observation of the earthquake swarm east off the Izu Peninsula in 1980, *Bull. Earthq. Res. Inst.*, **56**, 139–160, 1981 (in Japanese with English abstract).
- Morijiri, R., Geomagnetic total force anomaly and crustal structure of the Mineoka Belt in the southern part of Boso Peninsula, M.S. Thesis, Chiba Univ., 1988 (in Japanese).
- Morijiri, R., T. Fujiwara, S. Ogura, H. Kinoshita, and T. Nagao, Crustal structure and magnetic anomaly in southern part of Boso Peninsula, Chiba, Japan (abstract), *EOS Trans. AGU*, **71**, 942, 1990.
- Nakai, J., M. Komazawa, and Y. Okubo, Distribution of gravity anomalies and aeromagnetic anomalies in the Kanto District, *J. Geography*, **96**, 185–200, 1987 (in Japanese with English abstract).
- New Energy and Industrial Technology Development Organization (NEDO), Report of geothermal energy research, curie point depth survey of Japan (Kanto and Tokai district), 1983.
- Ogawa, Y. and K. Fujioka, Evolution of the plate boundary in the northeastern part of the Izu-arc—From the Mineoka Belt to the Sagami Trough—, *Chikyū*, **7**, 709–719, 1985 (in Japanese).
- Ogawa, Y. and H. Taniguchi, Ophiolitic melange in the forearc areas and the development of the Mineoka belt, *Sci. Rep. Dept. Geol., Kyushu Univ.*, **15**, 1–23, 1987 (in Japanese with English abstract).
- Ogawa, Y. and H. Taniguchi, Geology and tectonics of the MIURA-BOSO peninsulas and the adjacent area, *Modern Geology*, **12**, 147–168, 1988.
- Ogura, S., Analysis of geomagnetic anomaly in the southern part of Boso Peninsula by using prism model simulation, B.S. Thesis, Chiba Univ., 1990 (in Japanese).
- Okuma, S., M. Makino, and T. Nakatsuka, Two-layer model inversion of magnetic anomalies using pseudogravity and reduction to the pole: An application to the analysis of aeromagnetic anomalies over Izu-Oshima, *Butsuri-Tansa*, **42**, 82–96, 1989 (in Japanese with English abstract).
- Research Group for Active Faults of Japan, Active Faults in Japan: Sheet Maps and Investigations (revised edition), 1991.
- Saito, S., Stratigraphy of Cenozoic strata in the southern terminous area of Boso Peninsula, Central Japan, *Contr. Inst. Geol. Pal., Tohoku Univ.*, **93**, 1–37, 1992.
- Smith, W. H. F. and P. Wessel, Gridding with continuous curvature splines in tension, *Geophys.*, **55**, 293–305, 1990.
- Soh, W., K. T. Pickering, A. Taira, and H. Tokuyama, Basin evolution in the arc-arc Izu collision zone, Mio-Pliocene Miura group, central Japan, *J. Geol. Soc. London*, **148**, 317–330, 1991.
- Sugimura, A. and Y. Naruse, Changes in sea level, seismic upheavals and coastal terraces in the southern Kanto region, Japan (I), *Japan J. Geol. Geogr.*, **24**, 101–113, 1954.
- Sugimura, A. and Y. Naruse, Changes in sea level, seismic upheavals and coastal terraces in the southern Kanto region, Japan (II), *Japan J. Geol. Geogr.*, **26**, 165–176, 1955.
- Taira, A., H. Tokuyama, and W. Soh, Accretion tectonics and evolution of Japan, in *The Evolution of Pacific Ocean Margins*, edited by Zibben-Averaham, pp. 100–123, Oxford Univ. Press, New York, Oxford, 1989.
- Takigami, Y., I. Kaneoka, and M. Hirano, K-Ar and Ar-Ar dating on ophiolites from Mineoka, *Bull. Volcanol. Soc. Japan*, **25**, 308, 1980.
- Tonouchi, S. and K. Kobayashi, Paleomagnetic and geotectonic investigation of ophiolite suits and surrounding rocks in south central Honshu, Japan, in *Accretion Tectonics in the Circum-Pacific Regions*, edited by M. Hashimoto and S. Uyeda, pp. 261–288, Terra Sci. Publ. Tokyo, 1983.
- Uchida T. and S. Arai, Petrology of ultramafic rocks from the Boso Peninsula and the Miura Peninsula, *J. Geol. Soc. Japan*, **84**, 561–570, 1978.
- Ueda, Y., H. Nakagawa, T. Hiraiwa, T. Asao, and R. Kubota, Gravity anomalies and derived subterranean structure on/around Tokyo bay and southern Kanto district, *Rep. Hydrographic Res.*, **22**, 179–206, 1987.
- Wessel, P. and W. H. F. Smith, Free software helps map and display data, *EOS Trans. AGU*, **72**, 441, 445–446, 1991.

---

T. Fujiwara (e-mail: toshi@jamstec.go.jp), H. Kinoshita (e-mail: jimmy@jamstec.go.jp), and R. Morijiri (e-mail: g8808@gsj.go.jp)